

## Original Research Communication

# The microglial $\alpha 7$ acetylcholine nicotinic receptor is a key element in promoting neuroprotection by inducing HO-1 via Nrf2

Esther Parada<sup>\*,1</sup>, Javier Egea<sup>\*,1,3</sup>, Izaskun Buendia<sup>1</sup>, Pilar Negredo<sup>1,2,4</sup>, Ana C. Cunha<sup>5</sup>, Silvia Cardoso<sup>5</sup>, Miguel P. Soares<sup>5</sup> and Manuela G. L ópez<sup>1,3</sup>.

<sup>1</sup>Instituto Te ófilo Hernando and Department of Pharmacology, School of Medicine, Universidad Autónoma de Madrid, Madrid, Spain.

<sup>2</sup>Instituto Universitario la Paz-IdiPaz. Universidad Autónoma de Madrid.

<sup>3</sup>Instituto de Investigación Sanitaria Hospital Universitario La Princesa-IP.

<sup>4</sup>Departament of Anatomy, Histology and Neuroscience, School of Medicine, Universidad Autónoma de Madrid, Madrid, Spain.

<sup>5</sup>Instituto Gulbenkian de Ciência, 2780-156 Oeiras, Portugal.

\* *These authors contributed equally to this work.*

**Running title:** microglial  $\alpha 7$  nAChRs control neuronal survival

**Key words:** nicotinic receptors, microglia, neuroprotection, ischemia

**Corresponding author:** Manuela G. Lopez  
Departamento de Farmacología, Facultad de Medicina,  
Universidad Autónoma de Madrid  
C/ Arzobispo Morcillo 4  
E-28029 Madrid. Spain  
E-mail: manuela.garcia@uam.es  
Phone: +34-914975386

Fax: +34-914973120

Word count: 5.554

References: 62

Grayscale illustrations: 5 (figs. 1, 3, 4, 5, 6)

Color illustrations: 2 (figs. 2, 7)

## ABSTRACT

**Aims.** We asked whether the neuroprotective effect of cholinergic microglia stimulation during an ischemic event acts via a mechanism involving the activation of nuclear factor erythroid 2-related factor 2 (Nrf2) and/or the expression of its target cytoprotective gene, heme oxygenase-1 (HO-1). Specifically, the protective effect of the pharmacologic alpha-7 nicotinic receptor ( $\alpha 7$  nAChR) agonist PNU282987 was analyzed in organotypic hippocampal cultures (OHCs) subjected to oxygen and glucose deprivation *in vitro* as well as in photothrombotic stroke *in vivo*.

**Results.** OHCs exposed to oxygen and glucose deprivation (OGD) followed by re-oxygenation, elicited cell death, measured by propidium iodide and MTT staining. Activation of  $\alpha 7$  nAChR by PNU282987, after OGD, reduced cell death, ROS production and TNF release. This was associated with induction of HO-1 expression; an effect reversed by  $\alpha$ -bungarotoxin and by tin protoporphyrin IX (SnPP). The protective effect of PNU282987 was lost in microglia-depleted OHCs as well as in OHCs from Nrf2 deficient *vs.* wild type mice, an effect associated with suppression of HO-1 expression in microglia. Administration of PNU282987 1 h after induction of photothrombotic stroke *in vivo* reduced infarct size and improved motor skills in *Hmox1<sup>lox/lox</sup>* mice, that express normal levels of HO-1 but not in *LysM<sup>Cre</sup>Hmox1<sup>Δ/Δ</sup>* in which HO-1 expression is inhibited in myeloid cells, including the microglia.

**Innovation.** This study suggests the participation of the microglial  $\alpha 7$  nAChR in the “brain cholinergic anti-inflammatory pathway”.

**Conclusion.** Activation of the  $\alpha 7$  nAChR/Nrf2/HO-1 axis in microglia regulates neuroinflammation and oxidative stress affording neuroprotection under brain ischemic conditions.

## INTRODUCTION

Ischemic damage results from a cascade of cellular and molecular events triggered by sudden lack of blood flow and subsequent reperfusion of the ischemic territory. Post-ischemic inflammation is characterized by an orderly sequence of events involving a rapid activation of microglial cells, followed by infiltration of various circulating leukocytes, including granulocytes (neutrophils), T cells and monocyte/macrophages that irrupt in the ischemic parenchyma because of blood-brain barrier (BBB) breakdown (23,30). The specific role of microglia in this pathological scenario remains controversial. Microglia activation has been linked to the up-regulation of pro-inflammatory cytokines such IL-1 $\beta$  and TNF, chemokines and reactive oxygen species (ROS), that contribute to tissue damage progression (18,37). There is also an increasing body of evidence demonstrating the protective role of microglia in stroke. Post-ischemic production of TGF- $\beta$  and IL-10 by microglia may facilitate tissue repair by exerting direct cytoprotective effects on surviving cells in the ischemic penumbra and promoting the resolution of inflammation (9,34). This notion is strongly supported by a recent study showing the beneficial effects of human microglia transplanted into rats subjected to experimental focal brain ischemia (40).

Nicotinic acetylcholine receptors (nAChRs) are a family of ligand-gated ion channels and are members of the Cys-loop receptor superfamily (35). Activation of the  $\alpha 7$  nAChR is protective against a wide variety of cytotoxic stimuli, such as glutamate (53), OGD (15), and kainic acid (50). In recent years, nAChRs were shown to regulate inflammation, in particular via the  $\alpha 7$  nAChR activation in macrophages (61) which regulates the 'cholinergic anti-inflammatory pathway' (26,28,48,61). Transcripts for nAChR subunits  $\alpha 7$ ,  $\alpha 3$ ,  $\alpha 5$  as well as  $\beta 4$  have been detected in multiple inflammatory cell types, including macrophages and microglia, the resident macrophages of the brain (16,47).

The transcription factor Nrf2 (nuclear factor-erythroid 2-related factor 2) is a master regulator of redox homeostasis (22). Nrf2 controls the expression of phase 2 enzymes that act in a cytoprotective manner against oxidative stress, including heme oxygenase-1 (HO-1) (2) and the catalytic subunit of glutamate cysteine ligase (GCL-c). HO-1 serves a vital metabolic function as the rate-limiting step in the oxidative catabolism of heme to generate carbon monoxide (CO), biliverdin, and ferrous iron (56); biliverdin is subsequently converted to bilirubin by biliverdin reductase. These three by-products and in particular CO has been related to cytoprotection (5) during ischemic injury (1) including cerebral ischemia (27,60,65). Moreover, CO regulates monocyte/macrophage activation (42), an effect associated with protection against different experimental models of disease (43,51). Induction of HO-1 expression by different nicotinic receptor agonists and its importance in the maintenance of anti-inflammatory effects has been recently reported (57). On the other hand, induction of GCL-c, the rate-limiting enzyme of the novo synthesis of glutathione (GSH), by melatonin increases the levels of GSH and protects against oxidative stress (58).

Although the participation of  $\alpha 7$  nAChR in the cholinergic anti-inflammatory pathway is well documented in the periphery (61), there is little evidence related to its participation in the CNS. In this context, we used a highly selective microglia-target toxin and the selective  $\alpha 7$  nAChR agonist PNU282987 to evaluate the neuroprotective and anti-neuroinflammatory effects of the microglial- $\alpha 7$  nAChRs. Furthermore, we used Nrf2 deficient (*Nrf2*<sup>-/-</sup>) mice and *LysM*<sup>Cre</sup>*Hmox1* <sup>$\Delta/\Delta$</sup>  mice to assess the participation of this transcription factor in the regulation of HO-1 in microglial cells and in the neuroprotective effect mediated by  $\alpha 7$  nAChR activation. We found that microglial- $\alpha 7$  nAChR activation is crucial in the neuroprotective effect afforded by PNU282987, an effect mediated via a mechanism involving Nrf2 activation and HO-1 expression.

## RESULTS

### Cell death induced by OGD in OHCs

We first established the experimental conditions required to test the protective role of the  $\alpha 7$  nAChR agonist PNU282987. To determine the optimum period of OGD and re-oxygenation, OHCs were subjected to 15 or 30 min of OGD followed by a 24 or 48 h re-oxygenation period. Cell death was measured in the CA1 subfield which is considered to be the most vulnerable to hypoxia/anoxia (63). OGD for 15 or 30 minutes increased cell death by 177-161% and 234-243%, as compared to normoxia, respectively. No significant differences were found between 24 and 48 h re-oxygenation, independently of the OGD periods applied (**Fig. 1**). We therefore selected 15 min OGD followed by 24 h re-oxygenation as the standard protocol to perform the following studies.

### Effect of post-OGD administration of the $\alpha 7$ nAChR agonist PNU282987 on OHC viability

To evaluate the protective properties of  $\alpha 7$  nAChR, OHCs were treated with the  $\alpha 7$  nAChR agonist PNU282987 at different concentrations (1, 3 and 10  $\mu$ M) during the 24 h re-oxygenation period (see protocol in **Fig. 2A**). OGD (15 min) followed by re-oxygenation (24h) increased cell death as assessed by PI fluorescence in CA1 (compare basal condition in **Fig. 2B** with **Fig. 2C**). Post-OGD treatment with increasing concentrations of PNU282987 reduced PI staining (**Fig. 2D, 2E and 2F**). PNU282987 significantly reduced cell death measured as PI uptake at the concentrations of 10  $\mu$ M ( $110 \pm 10$  %) and 30  $\mu$ M ( $142 \pm 12$  %) in comparison to OHCs subjected to OGD alone ( $180 \pm 2$  %) (**Fig. 2G**).

Cell viability was also assessed by the colorimetric determination of MTT reduction. Considering cell viability in basal OHCs as 100 %, OGD reduced cell viability by 40 %; under these experimental conditions, maximum protection offered by PNU282987 was also

achieved at 10  $\mu$ M (60 %; **Fig. 2H**). We therefore selected the concentration of 10  $\mu$ M to evaluate the protective mechanism of action of  $\alpha 7$  nAChR stimulation against OGD-induced toxicity in OHCs.

### **Participation of the $\alpha 7$ nAChR/Nrf-2/HO-1 axis in the neuroprotective effect of PNU282987**

Although it is accepted that PNU282987 is a selective  $\alpha 7$  nAChR agonist (19), we wanted to prove that the neuroprotective effect of PNU 282987 is mediated by this receptor. We used the protocol illustrated in **Fig. 2A** in the absence or presence of  $\alpha$ -bungarotoxin (BGT, 100 nM), a selective  $\alpha 7$  nAChR antagonist (**Fig. 3A**). Inhibition of cell death associated with OGD /re-oxygenation by PNU282987 was abrogated by BGT, suggesting that this protective effect is indeed mediated via  $\alpha 7$  nAChR activation.

In other models of oxidative stress injury, the neuroprotective effect of PNU282987 has been suggested to be mediated via a mechanism involving HO-1 (44). We tested the involvement of this heme catabolising enzyme under our experimental conditions. The protective effect of PNU282987 (10  $\mu$ M) was associated with a 2.2-fold increase in HO-1 expression, as detected by western blotting and as compared with untreated controls (**Fig. 3B**). This effect was reversed by BGT, suggesting that  $\alpha 7$  nAChR activation induces the expression of HO-1. Inhibition of cell death by PNU282987 was also abrogated by Tin (Sn) protoporphyrin-IX (SnPP, 3  $\mu$ M), an inhibitor of HO activity (**Fig. 3A**), corroborating the participation of HO-1 in the protective effect of PNU282987. We evaluated the induction of GCL-c, another phase II enzyme. As shown in **Fig. 3C**, PNU282987 (10  $\mu$ M) increased GCL-c expression by 1.6-fold, as compared with controls. This effect was inhibited by BGT and by SnPP, suggesting that  $\alpha 7$  nAChR activation induces the expression of phase II enzymes, presumably conferring neuroprotection against OGD.

Given that HO-1 expression is tightly regulated by Nrf2 (2) we set-up to determine the participation of this transcription factor in the protective effect of PNU282987. The neuroprotective effect of PNU282987 against OGD was lost in OHCs from *Nrf2*<sup>-/-</sup> vs. *Nrf2*<sup>+/+</sup> mice (**Fig 4A**). This was associated with the concomitant loss of HO-1 induction in OHC from *Nrf2*<sup>-/-</sup> vs. *Nrf2*<sup>+/+</sup> mice, treated in both cases with PNU282987 (**Fig. 4B**). This suggests that the protective effect of PNU282987 acts via a mechanism that involves the induction of HO-1 by Nrf2.

### Anti-oxidant and anti-inflammatory effect of PNU282987

There is accumulating evidence implicating ROS and inflammation as pivotal mediators of acute responses of the brain to ischemia and its chronic pathogenic progression (25,31). OGD (15 min) followed by reoxygenation (24h) doubled the amount of ROS (measured by H<sub>2</sub>DCFDA) produced in OHCs, as compared to control (**Fig. 5A**). PNU282987 (10  $\mu$ M) reduced ROS production significantly, as compared to untreated controls. This effect was blocked by SnPP and by BGT as well, suggesting that the anti-oxidant effect triggered upon  $\alpha$ 7 nAChR activation is mediated by a mechanism involving HO-1.

To test the effects of PNU282987 on the production of cytokines induced by OGD/re-oxygenation, TNF and IL-10 were quantified by ELISA in the culture media of OHCs. OGD (15 min) followed by reoxygenation (24 h) increased TNF secretion, as compared to control OHCs (477 $\pm$ 50 pg/ml vs 109 $\pm$ 22 pg/ml). Treatment of OHCs with PNU 282987 10  $\mu$ M reduced TNF release almost to control levels (163  $\pm$  22 pg/ml). This inhibitory effect was prevented by SnPP (3  $\mu$ M) as well as by BGT (100 nM) (429  $\pm$  59 pg/ml; 377  $\pm$  82 pg/ml respectively). We did not observe changes in IL10 secretion in any of the conditions tested (data not shown). These results suggest that  $\alpha$ 7 nAChR activation inhibits the production of proinflammatory cytokines, TNF, via a mechanism involving the expression of HO-1.



## Participation of microglia in HO-1 induction and neuroprotection induced by PNU282987 against OGD

PNU282987 induced by 1.5 fold the expression of HO-1 in isolated microglial cells, as assessed by western blot (**S2**). Microglia depletion from OHC using Mac1-sap (39) was confirmed by IBA-1 staining (**Fig. 6A-B**) and was associated with increased cell death after OGD, in comparison to control OHCs. The protective effect of PNU282987 against OGD was impaired in microglia-depleted OHCs, as compared to non-depleted OHCs (**Fig. 6C**). Induction of HO-1 expression by PNU282987 was also reduced in microglia-depleted OHCs, as compared to control OHCs (**Fig. 6D**). This shows that  $\alpha 7$  nAChR activation in microglia induces the expression of HO-1 in microglia.

## PNU282987 reduces cortical infarct volume through the induction of HO-1 expression

We used the photothrombotic model of stroke in mice to evaluate whether the protective effects of PNU282987 acts under brain ischemic conditions *in vivo* (10). Following the protocol shown in **Fig. 7A**, ischemia induced by photothrombosis caused a mean cortical infarct volume of  $15.7 \pm 0.9$  %. Administration of PNU282987 (10 mg/kg), 1 h post-photothrombosis, reduced infarct volume by 40 % ( $9.4 \pm 0.4$  %). Administration of ZnDPBG (10 mg/kg), a potent HO inhibitor which crosses the blood brain barrier (24), did not alter infarct volume but prevented the neuroprotective effect of the  $\alpha 7$  nAChR agonist PNU282987 to  $14.6 \pm 0.8$  % (**Fig. 7B**).

To establish conclusively the involvement of HO-1, we compared the protective effect of PNU282987 against ischemia induced by photothrombosis in *Hmox1*<sup>lox/lox</sup> mice, expressing normal levels of HO-1 vs. *LysM*<sup>Cre</sup>*Hmox1*<sup>Δ/Δ</sup> in which HO-1 expression is inhibited specifically in myeloid cells (see methods and **S1**), including in the microglia. PNU282987

reduced infarct volume by 38 % in *Hmox1<sup>lox/lox</sup>* mice, as compared to untreated *Hmox1<sup>lox/lox</sup>* mice. Reduction in the infarct volume correlated with improved motor coordination measured by hindpaw slips in the beam walking test (**Fig. 7E**). In contrast, PNU282987 failed to reduce infarct volume or to improve motor coordination in *LysM<sup>Cre</sup>Hmox1<sup>Δ/Δ</sup>* mice (**Fig. 7C, 7D and 7E**). This reveals that expression of HO-1 in the myeloid compartment, and presumably in the microglia, is essential to support the neuroprotective effect of  $\alpha 7$  nAChR against brain ischemia induced by photothrombosis.

## DISCUSSION

In the present study, we provide experimental evidence *in vitro* as well as *in vivo* pointing to the crucial role of microglia in the neuroprotective effect afforded by the selective  $\alpha 7$  nAChR agonist PNU282987 against brain ischemia. Although there is convincing evidence that  $\alpha 7$  nAChR activation in macrophages exerts anti-inflammatory effects mediating the so called cholinergic anti-inflammatory pathway (61), few studies have addressed specifically whether this effect is also exerted in microglia, the resident macrophages of the brain. We provide evidence that  $\alpha 7$  nAChR activation induces the expression of HO-1 in microglia, which is required to support the neuroprotective effect of PNU282987 against brain ischemia. This notion is supported by the following independent observations i) PNU282987 induces HO-1 expression at the concentration that afforded maximum protection against brain ischemia, ii) The protective effect of PNU282987 is lost by inhibition of HO activity (**Fig. 2 and 3**), iii) Induction of HO-1 by PNU282987 is ablated by deletion of the transcription factor Nrf2 (**Fig. 4**), iv) The protective effect of PNU282987 is reversed by microglia deletion, an effect associated with loss of HO-1 expression (**Fig. 6**), and v) The protective effect of PNU282987 is ablated by specific deletion of HO-1 in myeloid cells, including the microglia (**Fig. 7**).

Signaling through nAChRs plays an important role in various processes such as neurite outgrowth, control and synthesis of neurotrophic factors, neuroprotection (20) as well as in the regulation of inflammation (48,61). Moreover, signaling via  $\alpha 7$  nAChR protects against neuronal death in different models of hemorrhagic brain injury (13,29). We have also previously shown that  $\alpha 7$  nAChR activation is protective in different *in vitro* models of ischemia/reoxygenation (15,44). Most of these studies have focused their attention on neuronal nicotinic receptors; while the participation of nAChRs in other brain cells like astrocytes and microglia has been less studied. The results obtained in the present work indicate that  $\alpha 7$  nAChRs expressed in microglia are key elements in promoting the protective effect of PNU282987. This notion is supported by the observation that the selective  $\alpha 7$  nAChR antagonist  $\alpha$ -bungarotoxin, prevented the neuroprotective effect and the induction of phase II enzymes (HO-1 and GCL-c) by PNU282987, and hence the reduction of ROS production and TNF release (**Fig 5**). Moreover, the protective effect of PNU282987 against brain ischemia is reduced by 70 % upon microglia deletion (**Fig. 6**). These observations strongly suggest that the “cholinergic anti-inflammatory pathway” described for peripheral macrophages, as controlling systemic inflammation, may have a brain counterpart, where microglia, the resident macrophages of the brain regulate inflammation via activation of the  $\alpha 7$  nAChRs.

Recent findings have elucidated the cellular signaling pathways and molecular mechanisms that mediate adaptive stress response which typically involve the synthesis of various stress resistance proteins as the products of “vitagenes”, a group of genes strictly involved in preserving cellular homeostasis during stressful conditions (6). The vitagene family is composed of the heat shock proteins (Hsp) HO-1/Hsp32, Hsp70, Hsp60, by the thioredoxin system and by sirtuin proteins. Nrf-2 is a master regulator of cellular redox homeostasis, controlling the expression of different genes that modulate cellular redox status

and inflammation (Phase II enzymes) including HO-1 (22). Induction of HO-1 expression has generally been considered to provide an adaptive cytoprotective response against the toxicity of oxidative stress (17,45,59). *Hmox1* deficient mice develop chronic inflammatory lesions that are similar to the ones observed in individuals lacking HO-1 expression (64). Hence, compounds targeting the vitagene network, could be a novel approach to delay various alterations in cells, tissues and organs and potentially prevent and treat many different diseases, such as ischemia. The mechanisms regulating the salutary effects of HO-1 remain however to be fully established (52).

The protective effect of PNU282987 acts via activation of Nrf2, as demonstrated by the loss of this protective effect in OHCs from *Nrf2*<sup>-/-</sup> mice (**Fig. 4A**). This effect is associated with inhibition of HO-1 expression in microglial cells from OHCs *Nrf2*<sup>-/-</sup> vs *Nrf2*<sup>+/+</sup> (**Figs. 4B and S2**). Recently, it has been hypothesized that pharmacological modulation of Nrf2 restores the cellular redox state through the expression of antioxidant phase II enzymes, down-modulating the pathological neuroinflammatory response of reactive microglia (21). Heme degradation by HO-1 in microglia generates CO (33), a gasotransmitter that can inhibit NADPH oxidase (55), the main enzyme responsible for microglial ROS production (4) promoting microglial activation during neuroinflammation (8). PNU282987 reduces ROS production as well as TNF release induced by brain ischemia, an effect mediated by the induction of HO-1 expression via  $\alpha 7$  nAChR signaling (**Fig. 5A and 5B**). This corroborates the importance of the Nrf-2/HO-1 system in the control of cellular redox state and modulation of the neuroinflammatory responses to ischemia. We infer that nAChR signaling modulates microglia activation via a mechanism mediated by Nrf2/HO-1, which inhibits ROS production.

Microglia has historically been viewed as immunocompetent cells that respond to inflammation by acting as antigen presenting cells or secreting cytokines. The specific role of

microglia in post-ischemic inflammation remains controversial. Resident microglia are activated rapidly in response to brain injury, within minutes of ischemia onset, and produce pro-inflammatory mediators, such as TNF and IL-1 $\beta$ , which exacerbate brain damage (18,37). Our data shows that cell death induced by OGD was significantly higher in microglia-depleted OHCs compared to non-depleted slices (**Fig. 6**). Hence, in our model, microglial cells have a protective role in the brain against ischemic injury.

We found that expression of HO-1, presumably in the microglia, mediates the protective effect of PNU282987 against photothrombotic brain ischemia, as assessed in *Hmox1*<sup>lox/lox</sup> mice, expressing normal levels of HO-1 vs. *LysM*<sup>Cre</sup>*Hmox1* <sup>$\Delta/\Delta$</sup>  in which HO-1 expression is inhibited specifically in myeloid cells, including in the microglia. Together with the data obtained in the OHC model, this suggests that expression of HO-1 by microglia is important to resolve the oxidative stress and neuroinflammation and most important, to stop the progression of cell death induced by an ischemic episode. This is in line with the notion, that microglia plays a central role in the regulation of brain ischemia and excitotoxic injury (32,40,41). We propose that pharmacologic modulation of HO-1 in microglia may be considered as a potential strategy against brain ischemia-induced injury (62).

## INNOVATION

We demonstrate the role of microglial  $\alpha 7$  nAChR in providing neuroprotective and anti-inflammatory actions under brain ischemia conditions by a mechanism that implicates the induction of HO-1 expression via Nrf2 activation. Our data supports the notion that microglial  $\alpha 7$  nAChR might be targeted therapeutically to modulate the “brain cholinergic anti-inflammatory pathway”.

## MATERIALS AND METHODS

### *Animals and preparation of organotypic slice cultures (OHCs)*

Organotypic slice cultures (OHC) were conducted on 8-10 day-old Sprague Dawley rats or wild type C57BL/6 mice and Nrf2-knockout mice of the same littermates. Nrf2-knockout mice were kindly provided by Dr. Antonio Cuadrado (Department of Biochemistry, School of medicine, Universidad Autónoma de Madrid). All animal assays were carried out following the European Community Council Directive issued for these purposes and were approved by the Ethics Committee of the Facultad de Medicina, Universidad Autónoma de Madrid. Every effort was made to minimize the number of animals used and their suffering.

Cultures were prepared according to the methods described by Stoppini et al. (54) with some modifications. Briefly, 300  $\mu$ m-thick hippocampal slices were prepared from rat or mice pups using a McIlwain tissue chopper, and separated in ice-cold Hank's balanced salt solution (HBSS) composed of (mM): glucose 15,  $\text{CaCl}_2$  1.3, KCl 5.36, NaCl 137.93,  $\text{KH}_2\text{PO}_4$  0.44,  $\text{Na}_2\text{HPO}_4$  0.34,  $\text{MgCl}_2$  0.49,  $\text{MgSO}_4$  0.44,  $\text{NaHCO}_3$  4.1 HEPES 25; 100 U/ml penicillin and 0.100 mg/ml gentamicin. Approximately 4–6 slices were placed on Millicell-0.4  $\mu$ m culture insert (Millipore, Madrid, Spain) within each well of a six-well culture tray with media, where they remained for 7 days. The culture media, which consisted of 50% Minimal Essential Media, 25% Hank's balanced salt solution and 25% heat inactivated horse serum, were purchased from Life Technologies (Madrid, Spain). The medium was supplemented with 3.7 mg/ml D-glucose, 2 mmol/L L-glutamine and 2% of B-27 Supplement Minus antioxidants (Life Technologies, Madrid, Spain) and 100 U/ml penicillin. OHCs were cultivated in a humidified atmosphere at 37 °C and 5%  $\text{CO}_2$ , and the medium was changed twice a week.

### Mice

C57BL/6 *Nrf2*<sup>-/-</sup> (22) and *Hmox1*<sup>LoxP</sup> (38) mice were generated by the laboratory of Dr. Masayuki Yamamoto (Tohoku University Graduate School of Medicine) and obtained through the RIKEN BioResource Center (*Nrf2*<sup>-/-</sup> mouse/C57BL6J and B6J.129P2-Hmox1<tm1Mym>). C57BL/6 *LysM*<sup>Cre</sup> mice were generated by the laboratory of Dr. Forster (7) and obtained through the Jackson Laboratory (B6.129P2-Lyz2tm1(cre)If0/J Stock Number:004781). *LysM*<sup>Cre</sup>*Hmox1*<sup>Δ/Δ</sup> mice used in this study were generated at the Instituto Gulbenkian de Ciência from *LysM*<sup>Cre</sup>*Hmox1*<sup>Δ/Δ</sup> x *LysM*<sup>Cre</sup>*Hmox1*<sup>Δ/Δ</sup>. The *LysM*<sup>Cre</sup>*Hmox1*<sup>Δ/Δ</sup> offspring is homozygous for the *LysM*<sup>Cre</sup> allele. Mice were genotyped by PCR from genomic DNA using the following primers for the *Hmox1* allele (*Hmox1* wild type forward 5'-CTCACTATGCAACTCTGTTGGAGG-3', *Hmox1* wild type reverse 5'-GTCTGTAATCCTAGCACTCGAA-3' and *Hmox1*<sup>LoxP</sup> reverse 5'-GGAAGGACAGCTTCTTGTAGTCG-3') and for the *LysM*<sup>Cre</sup> allele (Mutant 5'-CCCAGA AATGCCAGATTACG-3', Common: 5'-CTTGGGCTGCCAGAATTTCTC-3' and Wild type 5'-TTACAGTCGGCCAGGCTGAC-3'). Mice were bred at the Instituto Gulbenkian de Ciência with food and water provided *ad libitum*. Mice were used at 6 to 12 weeks of age and littermates were used as controls.

### Thioglycollate-induced peritoneal macrophages

Briefly, mice received (i.p., 2mL) a 3 % thioglycollate solution (w/v) and macrophages were obtained by peritoneal lavage 5 days thereafter in phosphate buffered saline (PBS; 5mL).

Peritoneal macrophages were stained with an Alexa467 conjugated-anti-CD11b (M1/70; 1:50 dilution) mAb and non-specific Fc binding was inhibited using anti-FcγIII/II receptor antibody (2.4G2; 1:50 dilution) in PBS 2% FCS (20 min., 4 °C). After washing and centrifugation (PBS 2 % FCS; 666g, 2 min., 4 °C), cells were sorted as CD11b<sup>+</sup> for the

*Hmox1*<sup>lox/lox</sup> and as CD11b<sup>+</sup>DsRed<sup>+</sup> or CD11b<sup>+</sup>DsRed<sup>-</sup> for the *LysM*<sup>Cre</sup>*Hmox1*<sup>ΔΔ</sup>. Cells were collected and analyzed by flow cytometry (FACS Aria; BD Biosciences), using BD FACSDiva Software (BD Biosciences) for acquisition. Post-acquisition analysis was performed with FloJo software (Treestar).

### *RNA isolation and qRT-PCR*

Briefly, mRNA was isolated from CD11b<sup>+</sup>-sorted cells and extracted with the RNeasy Mini Kit (Qiagen). cDNA synthesis was performed from 0.3-0.5 μg of RNA using random hexamer primers (0.3 mg/reaction; Invitrogen), dNTPs (0.5 mM/reaction; Invitrogen) (5 min., 65 °C). 5x First Strand buffer (Invitrogen) was added in the presence of DTT (10 mM/reaction; Invitrogen) and RNase Out recombinant ribonuclease inhibitor (40 U/reaction; Invitrogen) (2 min., 42 °C). SuperScriptII reverse transcriptase (200 U/reaction; Invitrogen) was added completing a final volume of 20 μl (50 min., 42 °C; 15 min., 70 °C). 1 μL of cDNA was used for PCR reactions (10 μl) using the Power SYBRGreen PCR master mix (Applied Biosystems) and optimal primer concentrations (previously determined for each transcript). PCR products were detected by qRT-PCR (ABI-7900HT; Applied Biosystems) (2 min., 50 °C, 10 min., 95 °C, and 40 cycles of 15 sec at 95 °C, 1 min., 60 °C). Primers used to amplify mouse mRNA transcripts were designed using the Primer3 software (Whitehead Institute for Biomedical Research, Steve Rozen and Helen Skaletsky) according to the specifications of the ABI-7900HT equipment (Applied Biosystems) and are listed below: *Hmox1* 5'-AAGGAGGTACACATCCAAGCCGAG-3' and 5'-GATATGGTACAAGGAAGCCATCACCAG-3', Glyceraldehyde 3-phosphate dehydrogenase (*GAPDH*) 5'-AACTTTGGCATTGTGGAAGG-3' and 5'-ACACATTGGGGGTAGGAACA-3'. Transcript number was calculated from the Ct of each gene using a 2<sup>-ΔΔCT</sup> method (relative number) and normalizing results to *GAPDH*.



### *Oxygen–glucose deprivation in OHCs*

Oxygen–glucose deprivation was used as an *in vitro* model of cerebral ischemia. The inserts with slice cultures were placed in 1 mL of OGD-solution composed of (in mM): NaCl 137.93, KCl 5.36, CaCl<sub>2</sub> 2, MgSO<sub>4</sub> 1.19, NaHCO<sub>3</sub> 26, KH<sub>2</sub>PO<sub>4</sub> 1.18 and 2-deoxyglucose 11 (Sigma-Aldrich, Madrid, Spain). The cultures were then placed in an airtight chamber (Billups and Rothenberg, Del Mar, CA, USA) and were exposed to 5 min of 95 % N<sub>2</sub>/5 % CO<sub>2</sub> gas flow to ensure oxygen deprivation. After that, the chamber was sealed for 15 min at 37 °C. Control cultures were maintained for the same time under normoxic atmosphere in a solution with the same composition as that described above (OGD-solution) but containing glucose (15 mM) instead of 2-deoxyglucose. After the OGD period, the slice cultures were returned to their original culture conditions for 24 hours (re-oxygenation period).

### *Quantification of Cell Death in OHCs*

#### *- Quantification of viability by MTT*

Cell viability, virtually the mitochondrial activity of living cells, was measured using the quantitative colorimetric assay of MTT, as described previously (11) with some modifications. Briefly, 1 ml of the MTT labeling reagent, at a final concentration of 0.5 mg/ml, was added to the medium of each well at the end of the OGD-reoxygenation period or normoxic period and the plate was placed in a humidified incubator at 37 °C with 5 % CO<sub>2</sub> and 95 % air (v/v) for an additional 30 min. Then, the insoluble formazan was dissolved with dimethyl sulfoxide; the colorimetric determination of MTT reduction was measured at 540 nm. Control cells treated under normoxic conditions with vehicle were taken as 100% viability.

### - *Propidium iodide uptake*

Cell death was determined in the CA1 region by staining the OHCs with propidium iodide (PI). Thirty minutes before analyzing fluorescence, slices were incubated with PI (1 µg/ml) and Hoechst (5 µg/ml); Hoechst staining was used to normalize PI fluorescence with respect to the number of nuclei. Fluorescence was measured in a fluorescence inverted NIKON Eclipse T2000-U microscope. Wavelengths of excitation and emission for PI and Hoechst were 530 or 350, and 580 or 460 nm, respectively. Images were taken at CA1 at magnifications of 10X. Fluorescence analysis was performed using the Metamorph programme version 7.0. To calculate cell death, we divided the mean PI fluorescence by the mean Hoechst fluorescence, as previously described (14). Data were normalized with respect to control values that were considered as 1.

### *ROS measurement in OHCs*

To measure cellular ROS, we used the molecular probe H<sub>2</sub>DCFDA as previously described (44). Briefly, organotypic hippocampal slices were loaded with 10 µM H<sub>2</sub>DCFDA, which diffuses through the cell membrane and is hydrolyzed by intracellular esterases to the nonfluorescent form dichlorofluorescein (DCFH). DCFH reacts with intracellular H<sub>2</sub>O<sub>2</sub> to form dichlorofluorescein, a green-fluorescent dye. Fluorescence was measured in a fluorescence inverted NIKON Eclipse T2000-U microscope. Wavelengths of excitation and emission were 485 and 520 nm, respectively.

### *Determination of cytokine levels in the culture medium of OHCs*

Tumor necrosis factor (TNF) and interleukin-10 (IL-10) levels were measured by using specific enzyme-linked immunosorbent assay (ELISA) kits. Supernatant samples here

obtained at the indicated times and subjected to ELISA analysis according to the recommendations of the supplier (R&D Systems-bioNova, Madrid, Spain).

#### *Immunotoxic depletion of microglial cells in OHCs*

Hippocampal slices were cultured for 5 days and then exposed to 3 or 5 nM of the immunocomplex Mac1–sap (Advanced Targeting Systems, San Diego, CA, USA) for 7 days. At the end of this period, the slices were fixed with paraformaldehyde 4 % for immunohistochemistry. The OGD experiments in microglia-depleted OHCs were performed at the end of the immunotoxic treatments.

#### *Histochemistry for microglia*

The organotypic slice cultures (OHCs) were fixed with 4 % paraformaldehyde in 0.1 M phosphate buffer (PB, pH 7.4) and were subsequently cryoprotected for 2 days in 30 % sucrose in 0.1 M PB. Endogenous peroxidase was inactivated with 1 % hydrogen peroxide, the OHCs were then incubated in blocking solution (PBS, 10 % bovine serum albumin (BSA) and 10 % normal goat serum) for 1 h and rabbit- anti-IBA1 (Ionized calcium-Binding Adaptor molecule 1) was used as the primary antibody 1:1000 (Wako Chemicals, Rafer S.L, Madrid, Spain) overnight. Secondary antibody was biotinylated goat anti-rabbit (Vector Labs, Burlingame, CA, USA; 1:200; 2 h) and was dissolved in blocking solution. The OHCs were incubated in avidin-biotin peroxidase complex (Kit ABC Elite®, 1:250 in PBS; Vector Laboratories, Burlingame, CA, USA) for 2 h and reacted with diaminobenzidine (DAB, 0.05 %; Sigma, Germany) with H<sub>2</sub>O<sub>2</sub> (0.003 % of the stock 30 % solution). The intensity of the staining was checked every few minutes under a microscope, and when labeling was satisfactory the reaction was stopped by rinsing the OHCs with cold PB. After several washes with PB, the OHCs were dehydrated in ethanol, defatted with xylene and coverslipped with

DePeX. Negative controls for the specificity of the secondary antibody were prepared by omitting the primary antibody.

### *Immunoblotting and image analysis*

After treatments, slices were carefully separated from the inserts and lysed in 100  $\mu$ l ice-cold lysis buffer (1 % Nonidet P-40, 10 % glycerol, 137 mM NaCl, 20 mM Tris-HCl, pH 7.5, 1  $\mu$ g/ml leupeptin, 1 mM phenylmethylsulfonyl fluoride, 20 mM NaF, 1 mM sodium pyrophosphate, and 1 mM  $\text{Na}_3\text{VO}_4$ ). Protein (30  $\mu$ g) from this cell lysate was resolved by SDS-PAGE and transferred to Immobilon-P membranes (Millipore Corp., Billerica, MA, USA). Membranes were incubated with anti-HO-1 (1:1000; Chemicon, Temecula, CA, USA), anti-GCLc subunit (1:10000 generous gift from Dr Cuadrado A) or anti- $\beta$ -actin (1:100,000; Sigma). Appropriate peroxidase-conjugated secondary antibodies (1:10,000) were used to detect proteins by enhanced chemiluminescence. Different band intensities corresponding to immunoblot detection of protein samples were quantified using the Scion Image program. Immunoblots correspond to a representative experiment that was repeated 4-5 times with similar results.

### *Microglial cell culture*

Microglia were isolated using a mild trypsinization method as previously described (49) with brief modifications. Mixed glial cultures were prepared from cerebral cortices of 3-day-old Sprague Dawley rats. After mechanical dissociation, cells were seeded in DMEM/F12 with 20% of Fetal Bovine Serum (FBS) at a density of 300,000 cells/ml and cultured at 37  $^{\circ}\text{C}$  in humidified 5%  $\text{CO}_2$ /95 % air. Medium was replaced after 5 days *in vitro* (DIV) for DMEM/F12 with 10 % FBS. Confluency was achieved after 10–12 DIV. High enriched microglial cultures were obtained with a trypsin solution (0.25 % trypsin, 1 mM EDTA)

diluted 1:4 in DMEM-F12. This process resulted in the detachment of an upper layer of cells in one piece, and microglial cells were attached to the bottom of the well. A great majority of cells (99 %) were positive for CD11b, as judged by immunocytochemical criteria.

### *Photothrombotic Stroke model*

All animal assays were carried out following the European Community Council Directive issued for these purposes and were approved by the Ethics Committee of the Facultad de Medicina, Universidad Autónoma de Madrid. Every effort was made to minimize the number of animals used and their suffering. Mice were housed individually under controlled temperature and lighting conditions with food and water provided *ad libitum*. To induce ischemia, animals were anesthetized with 1.5 % isoflurane in oxygen under spontaneous respiration. Mice were then placed in a stereotaxic frame (David Kopf Instruments, Tujunga, CA, USA) and body temperature was maintained at  $37 \pm 0.5$  °C using a servo-controlled rectal probe heating pad (Cibertec, Madrid, Spain). A midline scalp incision was made, the skull was exposed with removal of the periosteum, and both bregma and lambda points were identified. A cold-light (Zeiss KL 1500 LCD, Jena, Germany) was centered using a micromanipulator at 0.2 mm posterior and 1.5 mm lateral to bregma on the right side using a fiber optic bundle of 2 mm in diameter. According to the Paxinos mouse brain atlas, the primary motor cortex, secondary motor cortex and primary somatosensory cortex (hindlimb and forelimb) are lying beneath this stereotaxic position. One milligram (0.1 ml) of the photosensitive dye Rose Bengal (Sigma-Aldrich, St. Louis, MO, USA) dissolved in sterile saline was injected i.p. and 5 min later the brains were illuminated through the intact skull for 20 min. After completion of the surgical procedures, the incision was sutured and the mice were allowed to recover.

### *Drug administration protocol*

Mice were randomly divided into 4 groups: subjected to ischemia and treated with 0.9 % NaCl sterile saline solution (ischemia control group), treated with 10 mg/kg PNU282987 dissolved in saline containing 5 % DMSO, treated with Zinc (III) deuteroporphyrin IX-2,4 biseth yleneglycol (ZnDPBG) dissolved in DMSO and diluted in normal saline at a dose of 10 mg/kg (12), or with the combination of PNU282987 and ZnDPBG at the concentrations mentioned above. PNU282987 and ZnDPBG treatments were given i.p after ischemia (1 h and 15 min respectively).

### *Measurement of infarct volume*

Animals were sacrificed by decapitation 24 hours after the ischaemic insult. The brains were quickly removed and coronally sectioned into 1mm-thick slices. For delineation of infarct area, the brain slices were incubated in a 2 % solution of triphenyltetrazolium chloride and then fixed in a buffered formalin solution, the unstained area was defined as infarcted tissue. Morphometric determination of cortical infarct volume was obtained using an unbiased stereological estimator of volume based on Cavalieri's principle (3).

### *Beam walk test (BWT)*

Motor coordination of mice was assessed 24 h after the photothrombotic stroke by measuring the number of contralateral hindpaw slips in the beam walk apparatus (36,46). This test takes place over 3 consecutive days: 2 days of training and 1 day of testing. In the BWT, mice have to go through a 520 mm beam with a flat surface of 10 mm width resting 50 cm above the table top on two poles. A black goal box (150 mm x 150 mm x 150 mm) is placed at the end of the beam as the finish point. The amounts of hindpaw slips that occur in the process were counted.

### *Statistics*

Data are given as mean  $\pm$  SEM. Differences between groups were determined by applying a one-way ANOVA followed by a Newman-Keuls post-hoc or two-way ANOVA followed by a Bonferroni post-hoc test when appropriate.

### **ACKNOWLEDGEMENTS**

This work was supported in part by grants from Spanish Ministry of Science and Innovation Ref. SAF2009-12150 and SAF2012-32223 and the Spanish Ministry of Health (Instituto de Salud Carlos III) RETICS-RD06/0026 to MGL. EP and IB have a pre-doctoral fellowship from the Spanish Ministry of Economy. We would also like to thank the Fundación Teófilo Hernando for its continued support. Funding: Fundação para a Ciência e Tecnologia (Portugal) grants to MPS: PTDC/BIA-BCM/101311/2008, PTDC/SAU-FCF/100762/2008, and PTDC/SAU-TOX/116627/2010) and European Community 6th Framework Grant LSH-2005-1.2.5-1 and 7th Framework Grant ERC-2011-AdG. 294709 – DAMAGECONTROL. Ana Cunha was supported by a fellowship within the project PTDC/SAU-FCF/100762/2008 awarded to MPS. We also thank Sofia Rebelo (Instituto Gulbenkian de Ciência) who was responsible for the management of animals and David Fdez Villa, responsible for the construction of the Beam walk apparatus

**Abbreviation list:**

BV; Biliverdin

CO; carbon monoxide

HO-1; hemoxygenase-1

MTT; 3-(4,5-Dimethylthiazol-2-yl)-2,5-diphenyltetrazolium bromide

nAChR; nicotinic acetylcholine receptor

NADPH; nicotinamide adenine dinucleotide phosphate

NOX; NADPH oxidase

Nrf2; nuclear factor-erythroid 2-related factor 2

OGD; oxygen and glucose deprivation

OHCs; organotypic hippocampal cultures

PI; propidium iodide

Reox; reoxygenation

ROS; reactive oxygen species

ZnDPBG; Zinc (III) deuteroporphyrin IX-2,4 biseth yleneglycol

SnPP; Tin (Sn) protoporphyrin-IX

IBA1; Ionized calcium-Binding Adaptor molecule 1

GCL-c, glutamate cysteine ligase catalytic subunit



## REFERENCES

1. Akamatsu Y, Haga M, Tyagi S, Yamashita K, Graca-Souza AV, Ollinger R, Czismadia E, May GA, Ifedigbo E, Otterbein LE, Bach FH, Soares MP. Heme oxygenase-1-derived carbon monoxide protects hearts from transplant associated ischemia reperfusion injury. *FASEB J* 18: 771-2, 2004.
2. Alam J, Stewart D, Touchard C, Boinapally S, Choi AM, Cook JL. Nrf2, a Cap'n'Collar transcription factor, regulates induction of the heme oxygenase-1 gene. *J Biol Chem* 274: 26071-8, 1999.
3. Avendano C, Roda JM, Carceller F, Diez-Tejedor E. Morphometric study of focal cerebral ischemia in rats: a stereological evaluation. *Brain Res* 673: 83-92, 1995.
4. Block ML, Zecca L, Hong JS. Microglia-mediated neurotoxicity: uncovering the molecular mechanisms. *Nat Rev Neurosci* 8: 57-69, 2007.
5. Brouard S, Otterbein LE, Anrather J, Tobiasch E, Bach FH, Choi AM, Soares MP. Carbon monoxide generated by heme oxygenase 1 suppresses endothelial cell apoptosis. *J Exp Med* 192: 1015-26, 2000.
6. Calabrese V, Cornelius C, Dinkova-Kostova AT, Iavicoli I, Di Paola R, Koverech A, Cuzzocrea S, Rizzarelli E, Calabrese EJ. Cellular stress responses, hormetic phytochemicals and vitagenes in aging and longevity. *Biochim Biophys Acta* 1822: 753-83, 2012.
7. Clausen BE, Burkhardt C, Reith W, Renkawitz R, Forster I. Conditional gene targeting in macrophages and granulocytes using LysMcre mice. *Transgenic Res* 8: 265-77, 1999.
8. Choi SH, Aid S, Kim HW, Jackson SH, Bosetti F. Inhibition of NADPH oxidase promotes alternative and anti-inflammatory microglial activation during neuroinflammation. *J Neurochem* 120: 292-301, 2012.
9. de Bilbao F, Arsenijevic D, Moll T, Garcia-Gabay I, Vallet P, Langhans W, Giannakopoulos P. In vivo over-expression of interleukin-10 increases resistance to focal brain ischemia in mice. *J Neurochem* 110: 12-22, 2009.
10. De Ryck M, Van Reempts J, Borgers M, Wauquier A, Janssen PA. Photochemical stroke model: flunarizine prevents sensorimotor deficits after neocortical infarcts in rats. *Stroke* 20: 1383-90, 1989.
11. Denizot F, Lang R. Rapid colorimetric assay for cell growth and survival. Modifications to the tetrazolium dye procedure giving improved sensitivity and reliability. *J Immunol Methods* 89: 271-7, 1986.
12. Duranski MR, Elrod JW, Calvert JW, Bryan NS, Feelisch M, Lefer DJ. Genetic overexpression of eNOS attenuates hepatic ischemia-reperfusion injury. *Am J Physiol Heart Circ Physiol* 291: H2980-6, 2006.
13. Duris K, Manaenko A, Suzuki H, Rolland WB, Krafft PR, Zhang JH.  $\alpha 7$  nicotinic acetylcholine receptor agonist PNU-282987 attenuates early brain injury in a perforation model of subarachnoid hemorrhage in rats. *Stroke* 42: 3530-6, 2011.
14. Egea J, Martin-de-Saavedra MD, Parada E, Romero A, Del Barrio L, Rosa AO, Garcia AG, Lopez MG. Galantamine elicits neuroprotection by inhibiting iNOS, NADPH oxidase and ROS in hippocampal slices stressed with anoxia/reoxygenation. *Neuropharmacology* 62: 1082-90, 2012.
15. Egea J, Rosa AO, Sobrado M, Gandia L, Lopez MG, Garcia AG. Neuroprotection afforded by nicotine against oxygen and glucose deprivation in hippocampal slices is lost in  $\alpha 7$  nicotinic receptor knockout mice. *Neuroscience* 145: 866-72, 2007.
16. Galvis G, Lips KS, Kummer W. Expression of nicotinic acetylcholine receptors on murine alveolar macrophages. *J Mol Neurosci* 30: 107-8, 2006.
17. Gozzelino R, Jeney V, Soares MP. Mechanisms of cell protection by heme oxygenase-1. *Annu Rev Pharmacol Toxicol* 50: 323-54, 2010.

18. Gregersen R, Lambertsen K, Finsen B. Microglia and macrophages are the major source of tumor necrosis factor in permanent middle cerebral artery occlusion in mice. *J Cereb Blood Flow Metab* 20: 53-65, 2000.
19. Hajos M, Hurst RS, Hoffmann WE, Krause M, Wall TM, Higdon NR, Groppi VE. The selective alpha7 nicotinic acetylcholine receptor agonist PNU-282987 [N-[(3R)-1-Azabicyclo[2.2.2]oct-3-yl]-4-chlorobenzamide hydrochloride] enhances GABAergic synaptic activity in brain slices and restores auditory gating deficits in anesthetized rats. *J Pharmacol Exp Ther* 312: 1213-22, 2005.
20. Hejmadi MV, Dajas-Bailador F, Barns SM, Jones B, Wonnacott S. Neuroprotection by nicotine against hypoxia-induced apoptosis in cortical cultures involves activation of multiple nicotinic acetylcholine receptor subtypes. *Mol Cell Neurosci* 24: 779-86, 2003.
21. Innamorato NG, Rojo AI, Garcia-Yague AJ, Yamamoto M, de Ceballos ML, Cuadrado A. The transcription factor Nrf2 is a therapeutic target against brain inflammation. *J Immunol* 181: 680-9, 2008.
22. Itoh K, Chiba T, Takahashi S, Ishii T, Igarashi K, Katoh Y, Oyake T, Hayashi N, Satoh K, Hatayama I, Yamamoto M, Nabeshima Y. An Nrf2/small Maf heterodimer mediates the induction of phase II detoxifying enzyme genes through antioxidant response elements. *Biochem Biophys Res Commun* 236: 313-22, 1997.
23. Jin R, Yang G, Li G. Inflammatory mechanisms in ischemic stroke: role of inflammatory cells. *J Leukoc Biol* 87: 779-89, 2010.
24. Johnson RA, Lavesa M, Askari B, Abraham NG, Nasjletti A. A heme oxygenase product, presumably carbon monoxide, mediates a vasodepressor function in rats. *Hypertension* 25: 166-9, 1995.
25. Jung JE, Kim GS, Chen H, Maier CM, Narasimhan P, Song YS, Niizuma K, Katsu M, Okami N, Yoshioka H, Sakata H, Goeders CE, Chan PH. Reperfusion and neurovascular dysfunction in stroke: from basic mechanisms to potential strategies for neuroprotection. *Mol Neurobiol* 41: 172-9, 2010.
26. Kawahara R, Yasuda M, Hashimura H, Amagase K, Kato S, Takeuchi K. Activation of alpha7 nicotinic acetylcholine receptors ameliorates indomethacin-induced small intestinal ulceration in mice. *Eur J Pharmacol* 650: 411-7, 2011.
27. Kim YS, Zhuang H, Koehler RC, Dore S. Distinct protective mechanisms of HO-1 and HO-2 against hydroperoxide-induced cytotoxicity. *Free Radic Biol Med* 38: 85-92, 2005.
28. Kox M, Pompe JC, Peters E, Vaneker M, van der Laak JW, van der Hoeven JG, Scheffer GJ, Hoedemaekers CW, Pickkers P. alpha7 Nicotinic acetylcholine receptor agonist GTS-21 attenuates ventilator-induced tumour necrosis factor-alpha production and lung injury. *Br J Anaesth* 107: 559-66, 2011.
29. Krafft PR, Altay O, Rolland WB, Duris K, Lekic T, Tang J, Zhang JH. alpha7 Nicotinic Acetylcholine Receptor Agonism Confers Neuroprotection Through GSK-3beta Inhibition in a Mouse Model of Intracerebral Hemorrhage. *Stroke* 43: 844-50, 2012.
30. Kreutzberg GW. Microglia: a sensor for pathological events in the CNS. *Trends Neurosci* 19: 312-8, 1996.
31. Lakhan SE, Kirchgessner A, Hofer M. Inflammatory mechanisms in ischemic stroke: therapeutic approaches. *J Transl Med* 7: 97, 2009.
32. Lalancette-Hebert M, Gowing G, Simard A, Weng YC, Kriz J. Selective ablation of proliferating microglial cells exacerbates ischemic injury in the brain. *J Neurosci* 27: 2596-605, 2007.
33. Lee S, Suk K. Heme oxygenase-1 mediates cytoprotective effects of immunostimulation in microglia. *Biochem Pharmacol* 74: 723-9, 2007.
34. Lehrmann E, Kiefer R, Christensen T, Toyka KV, Zimmer J, Diemer NH, Hartung HP, Finsen B. Microglia and macrophages are major sources of locally produced transforming growth factor-beta1 after transient middle cerebral artery occlusion in rats. *Glia* 24: 437-48, 1998.
35. Lester HA, Dibas MI, Dahan DS, Leite JF, Dougherty DA. Cys-loop receptors: new twists and turns. *Trends Neurosci* 27: 329-36, 2004.

36. Luong TN, Carlisle HJ, Southwell A, Patterson PH. Assessment of motor balance and coordination in mice using the balance beam. *J Vis Exp*, 2011.
37. Mabuchi T, Kitagawa K, Ohtsuki T, Kuwabara K, Yagita Y, Yanagihara T, Hori M, Matsumoto M. Contribution of microglia/macrophages to expansion of infarction and response of oligodendrocytes after focal cerebral ischemia in rats. *Stroke* 31: 1735-43, 2000.
38. Mamiya T, Katsuoka F, Hirayama A, Nakajima O, Kobayashi A, Maher JM, Matsui H, Hyodo I, Yamamoto M, Hosoya T. Hepatocyte-specific deletion of heme oxygenase-1 disrupts redox homeostasis in basal and oxidative environments. *Tohoku J Exp Med* 216: 331-9, 2008.
39. Montero M, Gonzalez B, Zimmer J. Immunotoxic depletion of microglia in mouse hippocampal slice cultures enhances ischemia-like neurodegeneration. *Brain Res* 1291: 140-52, 2009.
40. Narantuya D, Nagai A, Sheikh AM, Masuda J, Kobayashi S, Yamaguchi S, Kim SU. Human microglia transplanted in rat focal ischemia brain induce neuroprotection and behavioral improvement. *PLoS One* 5: e11746, 2010.
41. Neumann J, Gunzer M, Gutzeit HO, Ullrich O, Reymann KG, Dinkel K. Microglia provide neuroprotection after ischemia. *Faseb J* 20: 714-6, 2006.
42. Otterbein LE, Bach FH, Alam J, Soares M, Tao Lu H, Wysk M, Davis RJ, Flavell RA, Choi AM. Carbon monoxide has anti-inflammatory effects involving the mitogen-activated protein kinase pathway. *Nat Med* 6: 422-8, 2000.
43. Otterbein LE, Soares MP, Yamashita K, Bach FH. Heme oxygenase-1: unleashing the protective properties of heme. *Trends Immunol* 24: 449-55, 2003.
44. Parada E, Egea J, Romero A, del Barrio L, Garcia AG, Lopez MG. Poststress treatment with PNU282987 can rescue SH-SY5Y cells undergoing apoptosis via alpha7 nicotinic receptors linked to a Jak2/Akt/HO-1 signaling pathway. *Free Radic Biol Med* 49: 1815-21, 2010.
45. Poss KD, Tonegawa S. Reduced stress defense in heme oxygenase 1-deficient cells. *Proc Natl Acad Sci U S A* 94: 10925-30, 1997.
46. Quinn LP, Perren MJ, Brackenborough KT, Woodhams PL, Vidgeon-Hart M, Chapman H, Pangalos MN, Upton N, Virley DJ. A beam-walking apparatus to assess behavioural impairments in MPTP-treated mice: pharmacological validation with R-(-)-deprenyl. *J Neurosci Methods* 164: 43-9, 2007.
47. Rock RB, Gekker G, Aravalli RN, Hu S, Sheng WS, Peterson PK. Potentiation of HIV-1 expression in microglial cells by nicotine: involvement of transforming growth factor-beta 1. *J Neuroimmune Pharmacol* 3: 143-9, 2008.
48. Rosas-Ballina M, Ochani M, Parrish WR, Ochani K, Harris YT, Huston JM, Chavan S, Tracey KJ. Splenic nerve is required for cholinergic antiinflammatory pathway control of TNF in endotoxemia. *Proc Natl Acad Sci U S A* 105: 11008-13, 2008.
49. Saura J, Tusell JM, Serratosa J. High-yield isolation of murine microglia by mild trypsinization. *Glia* 44: 183-9, 2003.
50. Shin EJ, Chae JS, Jung ME, Bing G, Ko KH, Kim WK, Wie MB, Cheon MA, Nah SY, Kim HC. Repeated intracerebroventricular infusion of nicotine prevents kainate-induced neurotoxicity by activating the alpha7 nicotinic acetylcholine receptor. *Epilepsy Res* 73: 292-8, 2007.
51. Soares MP, Bach FH. Heme oxygenase-1: from biology to therapeutic potential. *Trends Mol Med* 15: 50-8, 2009.
52. Soares MP, Marguti I, Cunha A, Larsen R. Immunoregulatory effects of HO-1: how does it work? *Curr Opin Pharmacol* 9: 482-9, 2009.
53. Stevens TR, Krueger SR, Fitzsimonds RM, Picciotto MR. Neuroprotection by nicotine in mouse primary cortical cultures involves activation of calcineurin and L-type calcium channel inactivation. *J Neurosci* 23: 10093-9, 2003.
54. Stoppini L, Buchs PA, Muller D. A simple method for organotypic cultures of nervous tissue. *J Neurosci Methods* 37: 173-82, 1991.

55. Taille C, El-Benna J, Lanone S, Boczkowski J, Motterlini R. Mitochondrial respiratory chain and NAD(P)H oxidase are targets for the antiproliferative effect of carbon monoxide in human airway smooth muscle. *J Biol Chem* 280: 25350-60, 2005.
56. Tenhunen R, Marver HS, Schmid R. The enzymatic conversion of heme to bilirubin by microsomal heme oxygenase. *Proc Natl Acad Sci U S A* 61: 748-55, 1968.
57. Tsoyi K, Jang HJ, Kim JW, Chang HK, Lee YS, Pae HO, Kim HJ, Seo HG, Lee JH, Chung HT, Chang KC. Stimulation of alpha7 nicotinic acetylcholine receptor by nicotine attenuates inflammatory response in macrophages and improves survival in experimental model of sepsis through heme oxygenase-1 induction. *Antioxid Redox Signal* 14: 2057-70, 2011.
58. Urata Y, Honma S, Goto S, Todoroki S, Iida T, Cho S, Honma K, Kondo T. Melatonin induces gamma-glutamylcysteine synthetase mediated by activator protein-1 in human vascular endothelial cells. *Free Radic Biol Med* 27: 838-47, 1999.
59. Vile GF, Basu-Modak S, Waltner C, Tyrrell RM. Heme oxygenase 1 mediates an adaptive response to oxidative stress in human skin fibroblasts. *Proc Natl Acad Sci U S A* 91: 2607-10, 1994.
60. Vitali SH, Mitsialis SA, Liang OD, Liu X, Fernandez-Gonzalez A, Christou H, Wu X, McGowan FX, Kourembanas S. Divergent cardiopulmonary actions of heme oxygenase enzymatic products in chronic hypoxia. *PLoS One* 4: e5978, 2009.
61. Wang H, Yu M, Ochani M, Amella CA, Tanovic M, Susarla S, Li JH, Wang H, Yang H, Ulloa L, Al-Abed Y, Czura CJ, Tracey KJ. Nicotinic acetylcholine receptor alpha7 subunit is an essential regulator of inflammation. *Nature* 421: 384-8, 2003.
62. Weinstein JR, Koerner IP, Moller T. Microglia in ischemic brain injury. *Future Neurol* 5: 227-246, 2010.
63. Wilde GJ, Pringle AK, Wright P, Iannotti F. Differential vulnerability of the CA1 and CA3 subfields of the hippocampus to superoxide and hydroxyl radicals in vitro. *J Neurochem* 69: 883-6, 1997.
64. Yachie A, Niida Y, Wada T, Igarashi N, Kaneda H, Toma T, Ohta K, Kasahara Y, Koizumi S. Oxidative stress causes enhanced endothelial cell injury in human heme oxygenase-1 deficiency. *J Clin Invest* 103: 129-35, 1999.
65. Yang C, Zhang X, Fan H, Liu Y. Curcumin upregulates transcription factor Nrf2, HO-1 expression and protects rat brains against focal ischemia. *Brain Res* 1282: 133-41, 2009.

## FIGURE LEGENDS

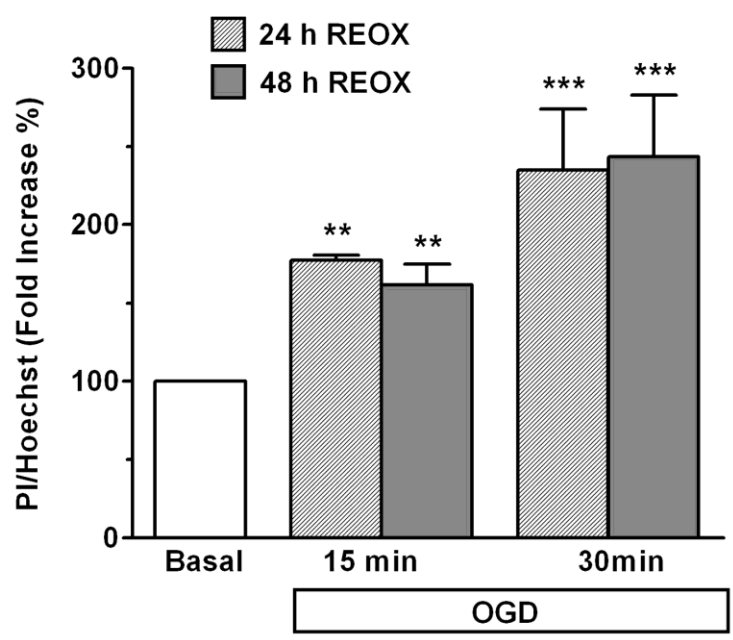


Figure 1

**Figure 1. Oxygen and glucose deprivation (OGD) increases cell death in organotypic hippocampal slices.** Cell death was labeled with propidium iodide (PI) fluorescence

corrected for the number of nuclei (Hoechst) in the CA1 subfield of rat organotypic slices after 15 or 30 min of oxygen and glucose deprivation (OGD) followed by 24 or 48 h of reoxygenation (REOX). Data are mean  $\pm$  SEM of seven independent experiments, \*\*\* $p$  < 0.001, \*\* $p$  < 0.01 with respect to the basal.

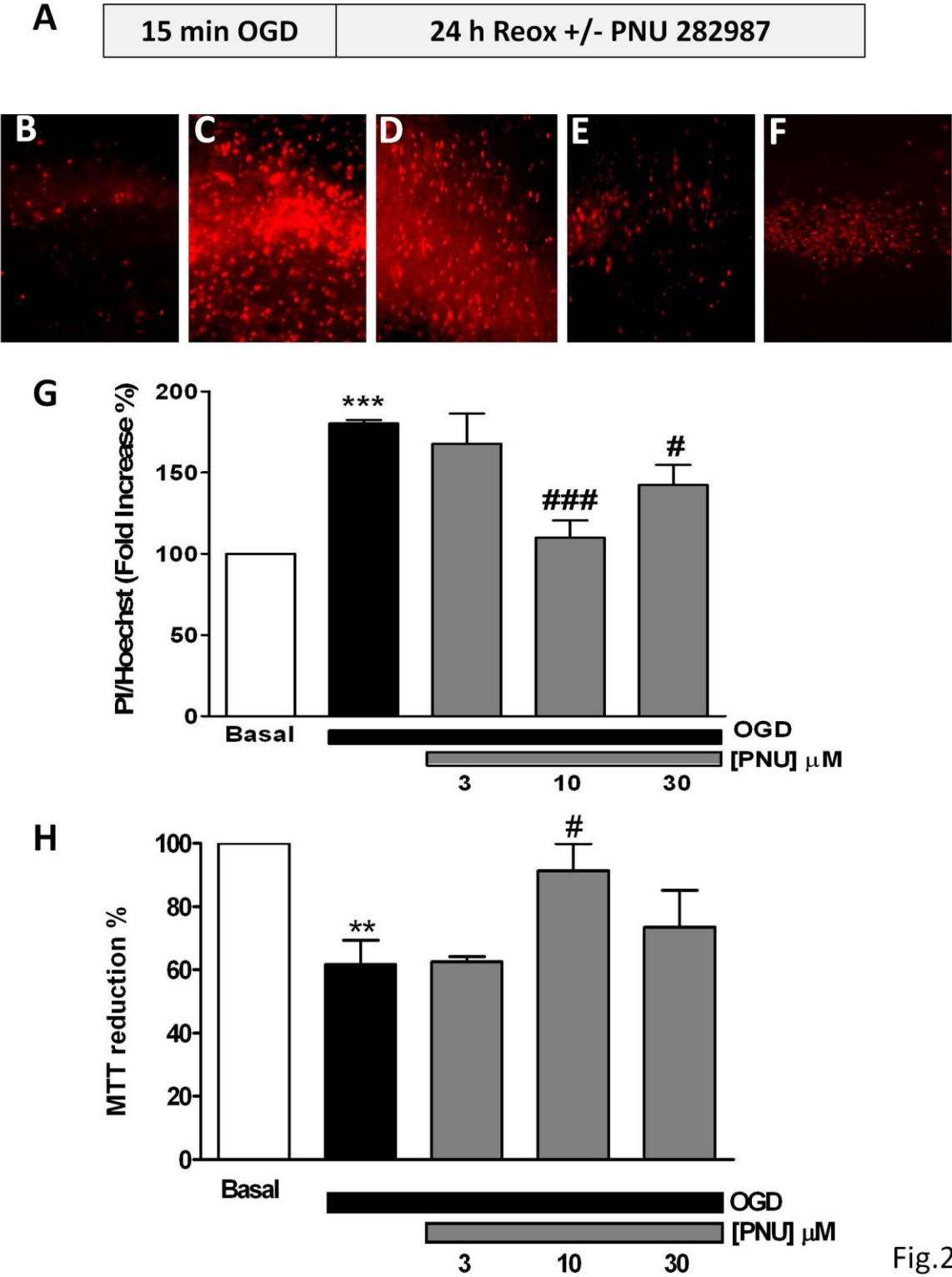
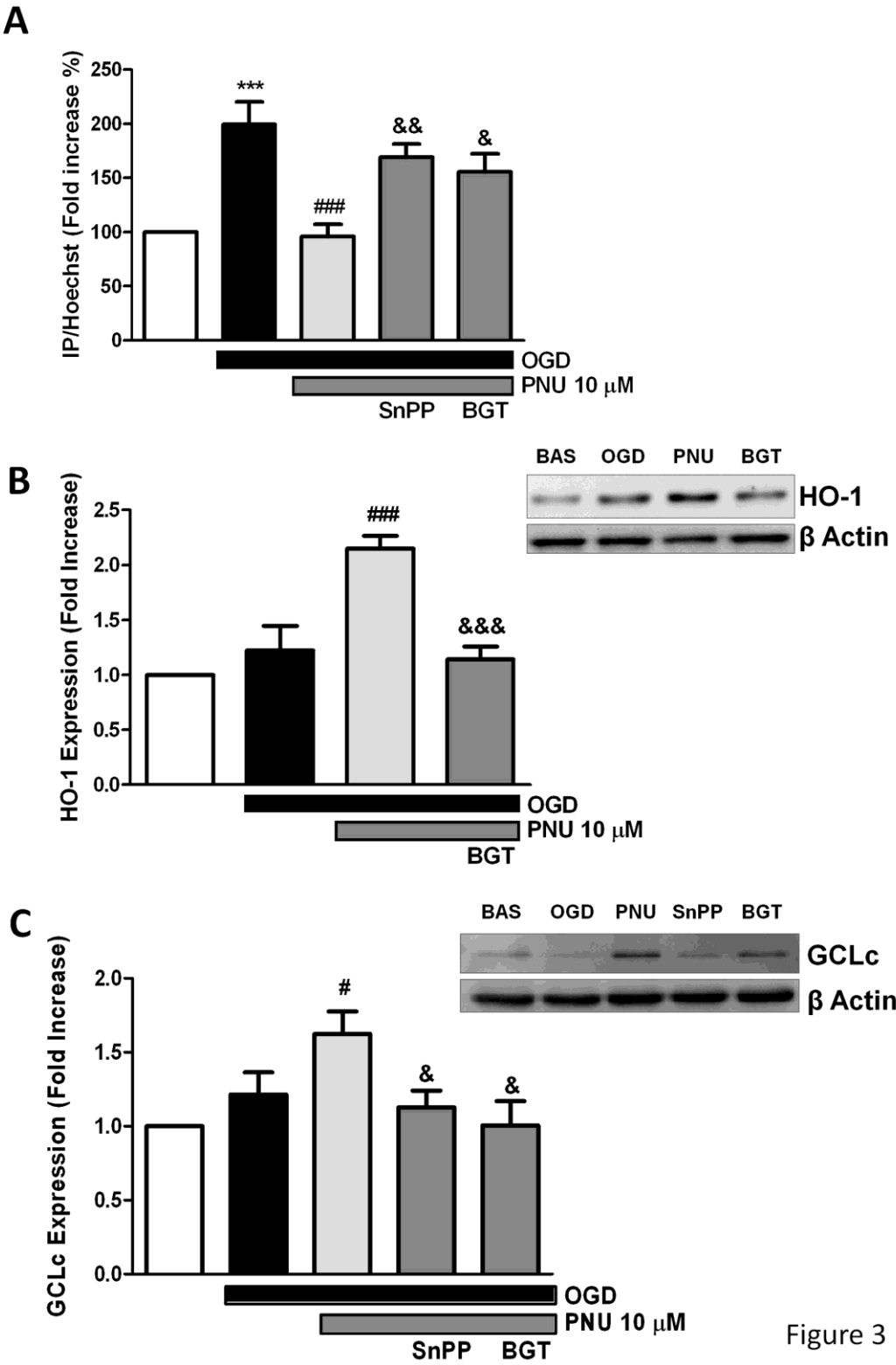


Fig.2

## Figure 2. Post-OGD treatment with the $\alpha 7$ nAChR agonist PNU282987 protects OHCs.

(A) Protocol used to elicit toxicity: OHCs were exposed for 15 min to OGD followed by 24 h in control solution (Reox). PNU282987, when used, was present during the 24 h Reox period. (B-F) Microphotographs (original magnification 10 $\times$ ) of the CA1 subfield loaded with PI are shown. (B) Untreated slice; (C) slice exposed to OGD for 15 min followed by 24 h with fresh medium, and slices treated for 24 h with PNU282987 after the OGD period at 3  $\mu$ M (D), 10  $\mu$ M (E) or 30  $\mu$ M (F). (G) Concentration-response curve of PNU282987 incubated for 24 h after the OGD period, measured as the relationship of PI/Hoechst fluorescence in the CA1 subfield. (H) Cell viability was measured by the MTT reduction activity of the organotypic slices under the same experimental conditions as in panel G. Values are expressed as mean  $\pm$  SEM of at least 5 independent experiments, \*\*\* $p$  < 0.001, \*\* $p$  < 0.01 compared to the basal. ### $p$  < 0.001, # $p$  < 0.05 with respect to OGD-treated slices in the absence of PNU282987.





**Figure 3. Protection elicited by post-OGD treatment with PNU282987 is mediated by  $\alpha 7$  nAChR, HO-1.** (A) OHCs were exposed to 15 min of OGD and then incubated with 10  $\mu$ M PNU282987 for 24 h in the presence or absence of 100 nM  $\alpha$ -bungarotoxin (BGT) and 3  $\mu$ M SnPP. Representative immunoblot of HO-1 (B) and GCLc (C) induction by PNU282987 in the absence or presence of 100 nM BGT and 3  $\mu$ M SnPP. The histogram represents the densitometric quantification of HO-1 and GCLc induction using  $\beta$ -actin for normalization. Values are mean  $\pm$  SEM of six experiments, \*\*\* $p$  < 0.001 compared with the untreated-slices, ### $p$  < 0.001, # $p$  < 0.05 with respect to the OGD-treated slices, \$\$\$ $p$  < 0.001, \$\$ $p$  < 0.01, \$ $p$  < 0.05 compared with the PNU282987 slices.

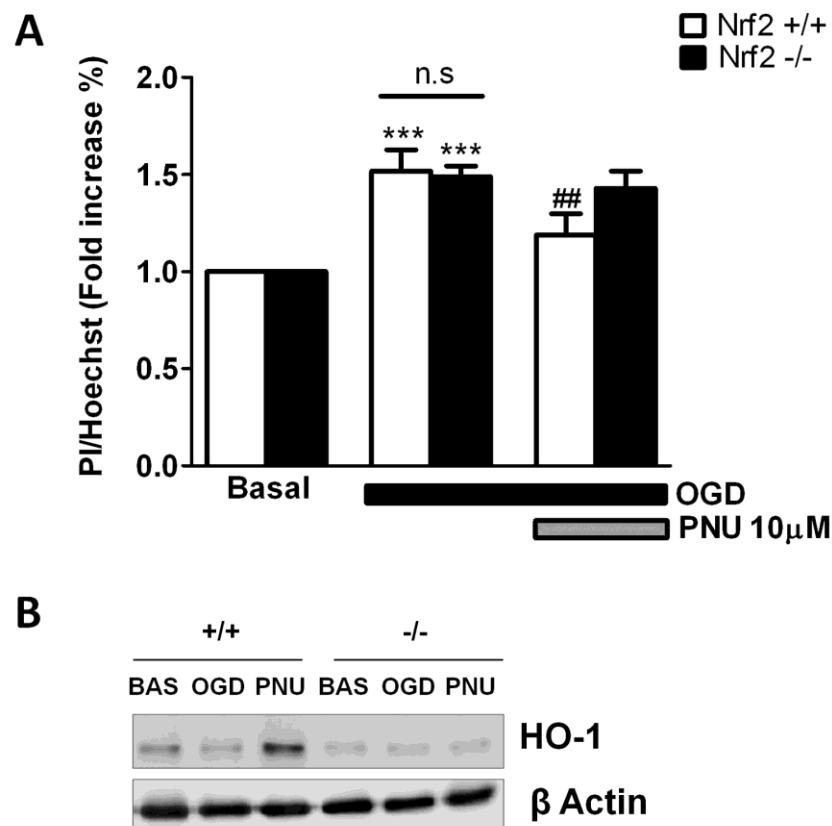


Fig. 4

**Figure 4. Protection elicited by post-stress treatment with PNU282987 is associated to the Nrf2/HO-1 axis.** (A) Following the protocol shown in Fig 2A, the protective effect of

post-OGD treatment with 10  $\mu$ M PNU282987 was tested in organotypic slices of Nrf2 wildtype (*Nrf2*<sup>+/+</sup>) and null mice (*Nrf2*<sup>-/-</sup>). Data are mean  $\pm$  SEM of six different experiments, \*\*\* $p$  < 0.001 compared with the untreated-slices, ## $p$  < 0.01 with respect to OGD. Panel (B) shows representative immunoblots of HO-1 induction under the different experimental conditions shown in A.

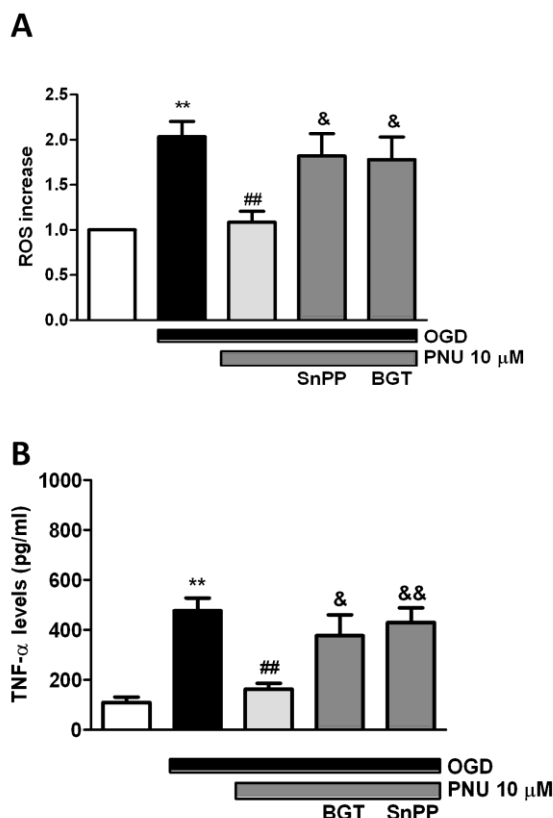


Figure 5

**Figure 5. PNU282987 reduces cellular ROS production and TNF- $\alpha$  release caused by OGD/Reox.** Panel (A) Effect of PNU282987 on ROS production elicited by OGD/Reox. OHCs were subjected to 15 min of OGD followed by 24 h of reoxygenation in the presence or absence of 10  $\mu$ M PNU282987, 100 nM BGT and 3  $\mu$ M SnPP. Panel (B) TNF release in OHCs supernatant measured under the same experimental conditions. Data are means  $\pm$  SEM of five independent experiments, \*\* $p < 0.01$  compared with the untreated-slices, ## $p < 0.01$  with respect to the OGD-treated slices, \$\$ $p < 0.01$ , \$ $p < 0.05$  compared with the PNU282987-treated slices.

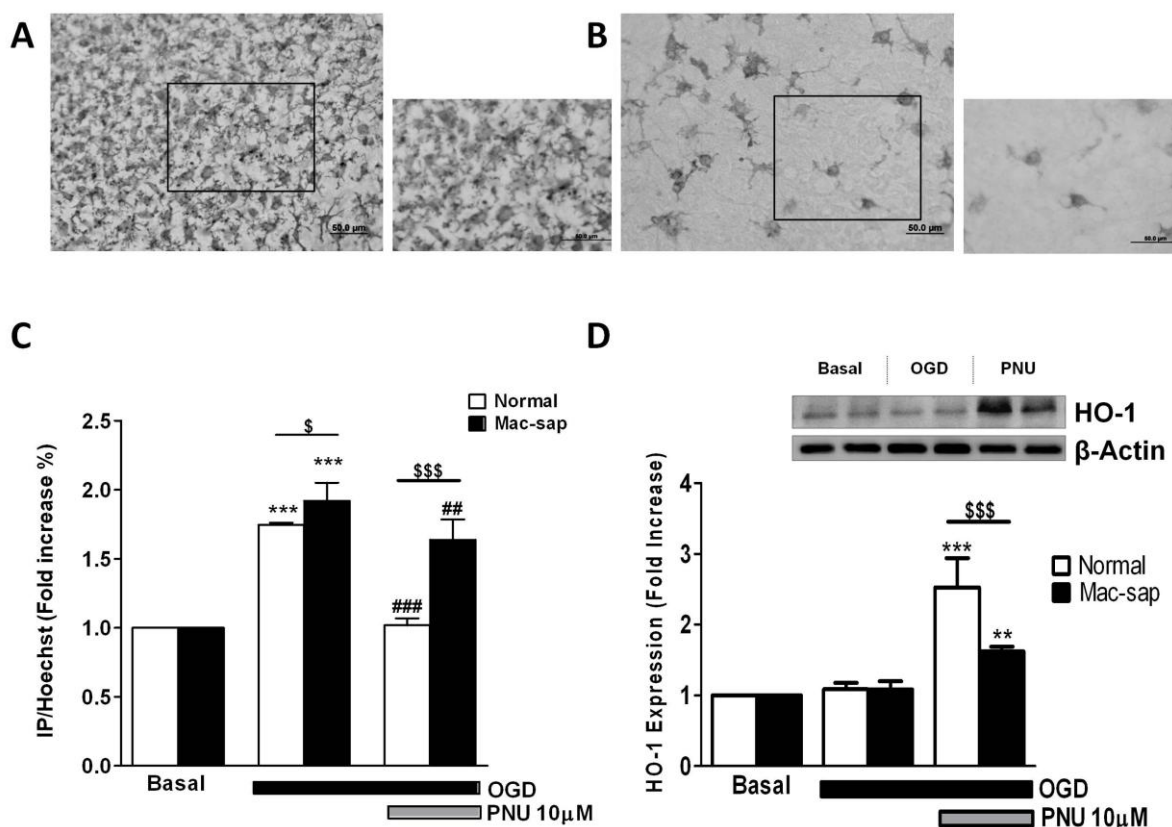


Figure 6

**Figure 6. Key role of microglia in the protective effect of PNU282987.** The top part of the figure illustrates immunohistochemical expression of the microglial marker IBA-1 in the CA1 pyramidal cell layer of OHCs. (A) shows an untreated slice and (B) slices treated with 5 nM of Mac1-sap, used to deplete microglia. To elicit toxicity, the protocol shown in Fig. 2 was followed. (C) Densitometric measurements of PI uptake in depleted and non-depleted microglia OHCs. (D) The top part of the figure shows a representative immunoblot of HO-1 induction under the same experimental conditions as shown in C; the bottom graph represents the densitometric quantification of HO-1, using  $\beta$ -actin for normalization. Data are means  $\pm$  SEM of six independent experiments, \*\*\* $p$  < 0.001, \*\* $p$  < 0.01 compared with the untreated-slices, ### $p$  < 0.001, ## $p$  < 0.01 with respect to the OGD-treated slices, \$\$\$ $p$  < 0.001, \$ $p$  < 0.05, depleted vs non-depleted slices.



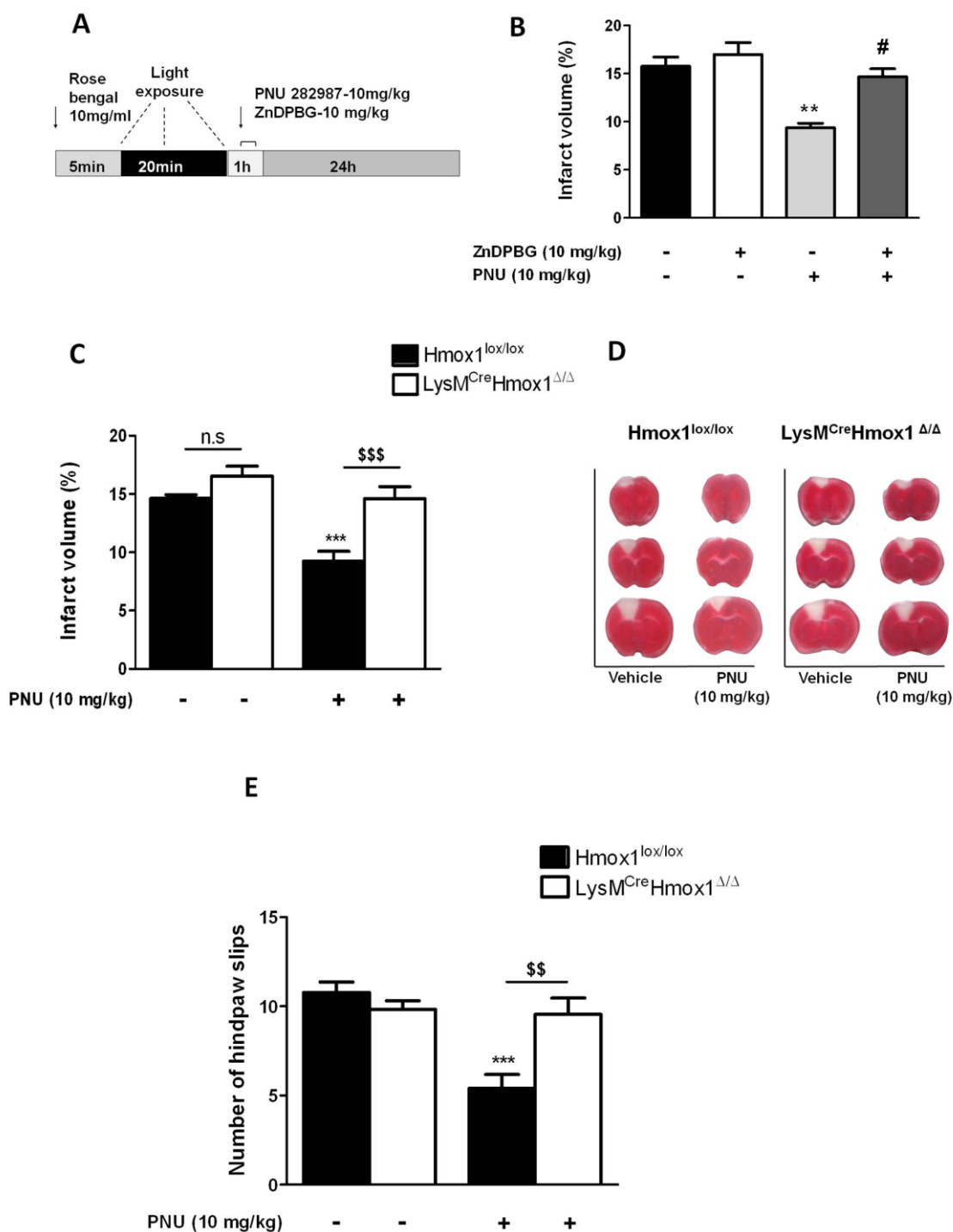


Figure 7

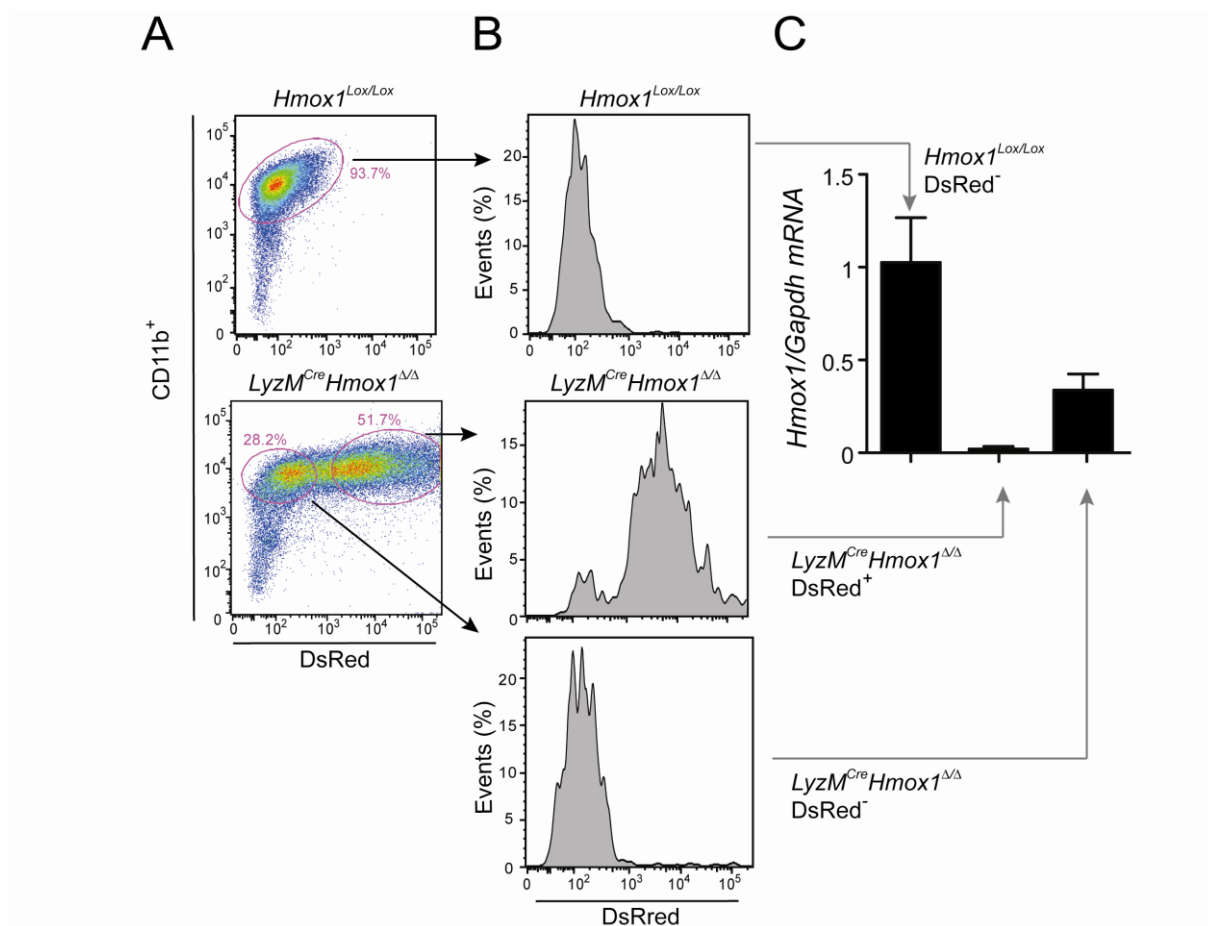
**Fig 7. PNU282987 reduces infarct volume and promotes functional recovery in mice subjected to photothrombotic stroke depending on HO-1 expression.** (A) Illustrates de



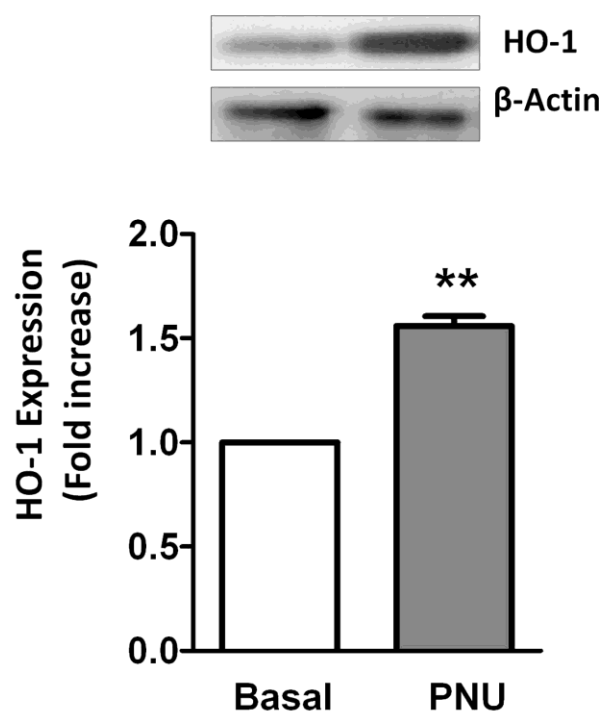
protocol used, in which PNU282987 (i.p at 10 mg/Kg) and/or ZnDPBG (i.p. at 10 mg/Kg) were administered 60 or 15 minutes after the thrombotic stroke, respectively. (B) Data are expressed as percentage (%) of cortical infarct volume in mice. Note that reduction of infarct in mice receiving PNU282987 was prevented by ZnDPBG. (C) Data are expressed as percentage (%) of cortical infarct volume in  $LysM^{Cre}Hmox1^{\Delta/\Delta}$  vs.  $Hmox1^{lox/lox}$  mice subjected to photothrombotic stroke and receiving or not PNU282987 (10 mg/Kg). (D) Representative photographs of the cortical infarcts of mice represented in C. (E) Motor skills analyzed with the Beam walk test 24 h after ischemia by quantification of hindpaw slips (see materials and methods) in the same animals as in C. Data is expressed as mean  $\pm$  SEM of 8 animals per group, in two independent experiments with the same trend.  $**p < 0.01$ , compared with ischemia plus saline group,  $***p < 0.001$  in comparison with  $Hmox1^{lox/lox}$  saline mice,  $$$$p < 0.001$ ,  $$$p < 0.01$   $LysM^{Cre}Hmox1^{\Delta/\Delta}$  vs.  $Hmox1^{lox/lox}$ .

**Supplemental data 1. HO-1 deletion in peritoneal CD11b<sup>+</sup> leukocytes from  $LysM^{Cre}Hmox1^{\Delta/\Delta}$  vs.  $Hmox1^{lox/lox}$  mice.** (A) Flow cytometry dot plots of thioglycollate-induced peritoneal CD11b<sup>+</sup> macrophages from C57BL/6  $Hmox1^{lox/lox}$  vs.  $LysM^{Cre}Hmox1^{\Delta/\Delta}$  mice, showing “gating strategy” used for sorting (red circles).  $Hmox1$  deletion is associated with expression of DsRed used in the targeting construct. (B) Cells were sorted (>95% purity) from  $Hmox1^{lox/lox}$  vs.  $LysM^{Cre}Hmox1^{\Delta/\Delta}$  mice as CD11b<sup>+</sup>DsRed<sup>-</sup> or CD11b<sup>+</sup> DsRed<sup>+</sup>. Data shown is representative of n=3 mice/genotype. (C) Expression of  $Hmox1$  mRNA analyzed by qRT-PCR in cells sorted in (B). Data is shown as mean  $\pm$  STD (n=3 mice/genotype). Notice total HO-1 deletion in CD11b<sup>+</sup>DsRed<sup>+</sup> cells from  $LysM^{Cre}Hmox1^{\Delta/\Delta}$  vs.  $Hmox1^{lox/lox}$  mice. Notice partial HO-1 deletion in CD11b<sup>+</sup>DsRed<sup>-</sup> cells from  $LysM^{Cre}Hmox1^{\Delta/\Delta}$  vs.  $Hmox1^{lox/lox}$  mice.

**Supplemental data 2. PNU282987 induced HO-1 expression in isolated microglia cultures.** Cells were treated with 10  $\mu$ M PNU282987 for 24h. Representative immunoblot of HO-1 induction (top), and densitometric quantification of HO-1 protein levels using  $\beta$ -actin for normalization (bottom). Data are means  $\pm$  SEM of three different cell cultures, \*\* $p < 0.01$  with respect to control cells.



HO-1 deletion in peritoneal CD11b<sup>+</sup> leukocytes from *LyzM*<sup>Cre</sup>*Hmox1*<sup>Δ/Δ</sup> vs. *Hmox1*<sup>lox/lox</sup> mice. (A) Flow cytometry dot plots of thioglycollate-induced peritoneal CD11b<sup>+</sup> macrophages from C57BL/6 *Hmox1*<sup>lox/lox</sup> vs. *LyzM*<sup>Cre</sup>*Hmox1*<sup>Δ/Δ</sup> mice, showing “gating strategy” used for sorting (red circles). *Hmox1* deletion is associated with expression of DsRed used in the targeting construct. (B) Cells were sorted (>95% purity) from *Hmox1*<sup>lox/lox</sup> vs. *LyzM*<sup>Cre</sup>*Hmox1*<sup>Δ/Δ</sup> mice as CD11b<sup>+</sup>DsRed<sup>-</sup> or CD11b<sup>+</sup> DsRed<sup>+</sup>. Data shown is representative of n=3 mice/genotype. (C) Expression of *Hmox1* mRNA analyzed by qRT-PCR in cells sorted in (B). Data is shown as mean ± STD (n=3 mice/genotype). Notice total HO-1 deletion in CD11b<sup>+</sup>DsRed<sup>+</sup> cells from *LyzM*<sup>Cre</sup>*Hmox1*<sup>Δ/Δ</sup> vs. *Hmox1*<sup>lox/lox</sup> mice. Notice partial HO-1 deletion in CD11b<sup>+</sup>DsRed<sup>-</sup> cells from *LyzM*<sup>Cre</sup>*Hmox1*<sup>Δ/Δ</sup> vs. *Hmox1*<sup>lox/lox</sup> mice.



Supplemental data 2

Supplemental data 2. PNU282987 induced HO-1 expression in isolated microglia cultures.

Cells were treated with 10  $\mu$ M PNU282987 for 24h. Representative immunoblot of HO-1

induction (top), and densitometric quantification of HO-1 protein levels using  $\beta$ -actin for

normalization (bottom). Data are means  $\pm$  SEM of three different cell cultures,  $**p < 0.01$  with respect to control cells.